Synthesis and Morphological Behavior of Silicon-Containing Triblock Copolymers for Nanostructure Applications

Apostolos Avgeropoulos,[†,‡] Vanessa Z-H Chan,[‡] Victor Y. Lee,[§] Don Ngo,[§] Robert D. Miller,[§] Nikos Hadjichristidis,*[,†] and Edwin L. Thomas*[,‡]

Department of Chemistry, University of Athens, Panepistimiopolis, 157 71 Zografou, Athens, Greece, Department of Materials Science, Massachusetts Institute of Technology, Cambridge, Massachusetts 02139, and IBM Almaden Research Center, 650 Harry Road, San Jose, California 95120

Received October 15, 1997. Revised Manuscript Received February 19, 1998

We report the synthesis of high molecular weight triblock copolymers of the type ABA and BAB, where A is polyisoprene (PI) and B is poly(pentamethyldisilylstyrene) (P(PMDSS)), respectively. The volume fraction of the minority component (PI) for the ABA copolymer was 0.33, while that for the BAB copolymer was 0.23. The synthesis procedure of the P(PMDSS) blocks corresponded to that of polystyrene (PS), and low polydispersity with targeted compositions were achieved. The morphology of the triblock copolymers was characterized by transmission electron microscopy (TEM) and digital Fourier transform patterns. From TEM and diffraction analysis, the ABA polymer exhibited the double gyroid cubic morphology, while the BAB polymer showed a P(PMDSS) spherical domain morphology. The double gyroid morphology is the first to be reported in a silicon-containing block copolymer and consists of two three-dimensionally continuous, interpenetrating but nonintersecting networks of PI in a matrix of P(PMDSS)). Preliminary oxidative studies using ozone or O_2-RIE on the tricontinuous phase show that nanoporous structures can be generated.

Introduction

Traditionally, high-resolution 2-D patterns have been generated by microlithographic techniques. However as the complexity of integrated circuits increases, so do the problems associated with using single-layer resists over chip topography. For this reason, a variety of multilayer resist schemes have been developed. The simplest of these utilizes a thin imageable layer coated over a thick planarizing polymer. After development, the high-resolution images from the top layer are transferred by oxygen reactive ion etching (O_2-RIE) using anisotropic etching techniques. Since most organic polymers containing C, H, N, O, etc. are rapidly etched by the aggressive oxygen plasma, considerable effort has been expended on the development of imageable polymers which form refractory oxides in an oxygen plasma (e.g. polymers containing Si, Ge, Sn, B, Ti, Al, etc).[2−6] Silicon-containing polymers are common and inexpensive; therefore, this element has received the most attention.[7] Such materials can form a thin layer of etch resistant SiO_x when exposed to an oxygen plasma. This layer is responsible for their extremely low etching rate relative to polymers containing only C, H, N, and O.[8] This etch selectivity provides the basis for most of the multilayer resist schemes involving pattern transfer. However, this selectivity may also be useful for the formation of structures in a heterogeneous polymer film where one of the phases contains silicon and the other does not, i.e., in a block copolymer. Since block copolymers can self-assemble into a variety of interesting morphologies which depend on the structure and composition of the individual blocks, employing silicon-containing block copolymers for pattern development and visualization should a promising route for the development of nanostructures.[9−11]

A number of studies on the synthesis of siloxane-based block copolymers for various applications have

* Author to whom correspondence should be addressed.
† University of Athens.
‡ Massachusetts Institute of Technology.
§ IBM Almaden Research Center.

(1) Thompson, L. F.; Willson, C. G.; Bowden, M. J., Eds. *Introduction to Microlithography*; American Chemical Society: Washington, DC, 1994; Chapter 4.
(2) Gabor, A. H.; Ober C. K. *Microelectronics Technology: Polymers for Advanced Imaging and Packaging;* ACS Symposium Series 614; American Chemical Society: Washington, DC, **1995**; Chapter 19.
(3) Hirao, A.; Ando, Y.; Nakahama, S. *Macromol. Symp.* **1995**, *95*, 293.
(4) Gabor, A. H.; Lehner, E. A.; Mao, G.; Schnegenburger, L. A.; Ober, C. K. *Chem. Mater.* **1994**, *6*, 927.
(5) Sugita, K.; Ueno, N. *Prog. Polym. Sci.* **1992**, *17*, 319.
(6) Miller, R. D.; Wallraff, G. *Adv. Mater. Optics Electronics* **1994**, *4*, 95.
(7) Chu, J; Rangarajan, P.; Adams, L. J.; Register, R. A. *Polymer* **1995**, *36* (8), 1569.
(8) Hartney, M. A.; Novembre, A. E.; Bates, F. S. *J. Vac. Sci. Tech B* **1985**, *3(5)*, 1346.
(9) Mansky, P.; Chaikin, P. M.; Thomas, E. L. *J. Mater. Sci.* **1995**, 30, 1987.
(10) Mansky, P.; Harrison, C. K.; Chaikin, P. M.; Register, R. A.; Yao, M. *Appl. Phys. Lett.* **1996**, *68* (18), 2586.
(11) Park, M.; Harrison, C.; Chaikin, P. M.; Register, R. A.; Adamson, D. H. *Science* **1997**, 276, 1401.

S0897-4756(97)00682-0 CCC: $15.00
Published on Web 07/22/1998

been reported.[12,13] For example, they have been studied for bilevel photoresists in image transfer processes.[14] In these cases, however, the siloxane block usually plays a passive role of providing an O_2-RIE etch barrier. Self-assembly is limited to the tendency of the low surface energy siloxane blocks to migrate to the air−film interface, thereby modifying the surface properties of the film. One intrinsic problem with most siloxane polymers is that they have very low T_g values, resulting in poor dimensional stability during processing without cross-linking.[15] In addition, for lithography, the range of self-assembled structures examined was limited, since the goals were primarily oxygen etch resistance and/or surface modification.

In addition to the siloxanes, silicon has been introduced into a variety of 1,3-diene block copolymers either through the use of silicon-containing monomers or by postpolymerization functionalization.[16] Regarding the latter, Ober et al.[2] have investigated the hydrosilylation of a number of poly(styrene)−poly(butadiene) or poly(styrene)−poly(isoprene) block copolymers. The viability of these polymers as electron beam resists was investigated. The O_2-RIE etch rate selectivity of the silylated block relative to polyimide was impressive (42:1). However, the stability of the functionalized butadiene copolymers was limited and the hydrosilylation of the isoprene phase of the block copolymers could not be driven to completion.

It is possible to use ozonolysis to oxidatively image these nanoporous structures. This is due to the very high selectivity of ozone between the polydienes and polymers which do not contain double bonds in the backbone. The use of ozone to produce nanoporous structures has been reported by various investigators.[17−20] In 1989, Lee et al.[21] were the first to make porous membranes from ozone etching out poly((4-vinylphenyl)dimethyl-2-propoxysilane)−poly(isoprene) block copolymers.

Anionic polymerization has traditionally been the route to well-defined block copolymers, although recent developments in living free radical copolymerization suggest considerable potential.[22] The anionic polymerization of *p*-trimethylsilylstyrene was reported by Chaumont et al.[23] and Yamzaki et al.[24] More recently, Hirao et al.[25] studied the anionic polymerization of styrene derivatives containing permethyl oligosilane substituents. These authors prepared triblock copolymers of the ABA type, where A is *p*-trimethylsilylstyrene and B is either styrene or isoprene. Recently, the same authors have reported the formation of block copolymers from a variety of oligosilyl-substituted styrenes and styrene.[26] Although monodisperse diblock copolymers of poly(pentamethyldisilylstyrene) P(PMDSS), whose structure is shown in Figure 1, and polystyrene (PS) were reported, the molecular weights were relatively low (M_w < 29 000) and morphology studies were not described.

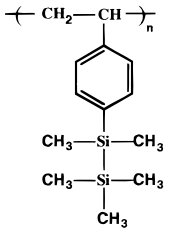

Figure 1. Chemical structure of poly(pentamethyldisilylstyrene).

In this paper, we describe the preparation of various high molecular weight, well-defined ABA and BAB triblock copolymers of *p*-pentamethyldisilylstyrene and isoprene and report on the interesting morphologies achieved by self-assembly. In these materials, the silicon is located in the high T_g ($T_g \sim 100$ °C), dimensionally stable block P(PMDSS). Since the silicon is already present in the monomer and is unaffected by the polymerization, no postpolymerization reactions are required. The copolymers were stable both in solution and in the solid state and no gelation was observed. The low T_g polyisoprene (PI) block ($T_g = -60$ °C) was chosen to both introduce reactive functionality for subsequent oxidative imaging (O_2-RIE or ozone) and to facilitate processing by techniques such as roll-casting.[27] It was anticipated that since the silicon-containing block has a weight percent of silicon higher than 10 wt %, which is the minimum necessary to form an etch barrier in an oxygen plasma, it would be possible to form nanostructures by selectively removing the isoprene block by either oxygen reactive ion etching, ozonolysis, or a combined route. By utilizing O_2-RIE, it will be possible to convert the silicon in the P(PMDSS) block to SiO_x, which should impart superior thermal and dimensional stability to these nanostructures as compared to a conventional organic polymer. Extensive work on both the reactive ion etching and ozonolysis of samples discussed in this paper as well as compositional variants expected to form P(PMDSS) cylinders in a PI matrix and PI cylinders in a P(PMDSS) matrix will be reported elsewhere.

Experimental Section

(a) Synthesis of the Monomer. *p*-Pentamethyldisilylstyrene was synthesized by a modified literature procedure.[28] In a 500 mL three-neck flask equipped with mechanical stirring, magnesium turnings (9.14 g, 381 mmol) in THF (100 mL) were

(12) Chu, J.; Rangarajan, P.; Adams, L. J.; Register, R. A. *Polymer* **1995**, *36* (8), 1569.
(13) Benrashid, R.; Nelson, G. L. *J. Polym. Sci. Part A: Polym. Chem.* **1994**, *32*, 1847.
(14) Hartney, M. A.; Novembre, A. E. *SPIE* **1985**, *539*, 90.
(15) Bushnell, L. P.; Gregor, L. V.; Lyons, C. F. *Solid State Technol.* **1986**, *29*, 133.
(16) Guo, X.; Rempel, G. L. *Macromolecules* **1992**, *25*, 883.
(17) Mansky, P.; Chaikin, P.; Thomas, E. L. *J. Mater. Science* **1995**, 30, 1987.
(18) Mansky, P.; Harrison, C. K.; Chaikin, P. M.; Register, R. A.; Yao, N.; *Appl. Phys. Lett.* **1996,** *68* (18), 2586.
(19) Park, M.; Harrison, C.; Chaikin, P. M.; Register, R. A.; Adamson, D. H. *Science* **1997,** *276*, 1401.
(20) Hashimoto, T.; Tsutsumi, K.; Funaki, Y. *Langmuir* **1997**, *13*, 6869.
(21) Lee, J−S.; Hirao, A.; Nakahama, S. *Macromolecules* **1989,** *22*, 2602.
(22) Hawker, C. J.; Elce, E.; Dao, J.; Volksen, W.; Russell, T. P.; Barclay, G. *Macromolecules* **1996**, *29*, 3876.
(23) Chaumont, P.; Beinert, G.; Herz, J. E.; Rempp, P. *Makromol. Chem.* **1982**, *183*, 1183.
(24) Yamazaki, N.; Nakahama, S.; Hirao, A.; Shiraishi, Y.; Phung, H. M. *Contemp. Top. Polym. Sci.* **1984**, *4*, 379.
(25) Hirao, A.; Nakahama S. *Prog. Polym. Sci.* **1992**, *17*, 283.
(26) Hirao, A.; Ando, Y.; Nakahama, S. *Macromol. Symp.* **1995**, *95*, 293.
(27) Albalak, R. J.; Thomas, E. L. *J. Polym. Sci. Part B: Polym. Phys.* **1993**, *31*, 37.
(28) Kawakami, Y.; Hisada, H.; Yamashita U. *J. Polym. Sci., Polym. Chem.* **1988**, *26*, 1307.

Scheme 1

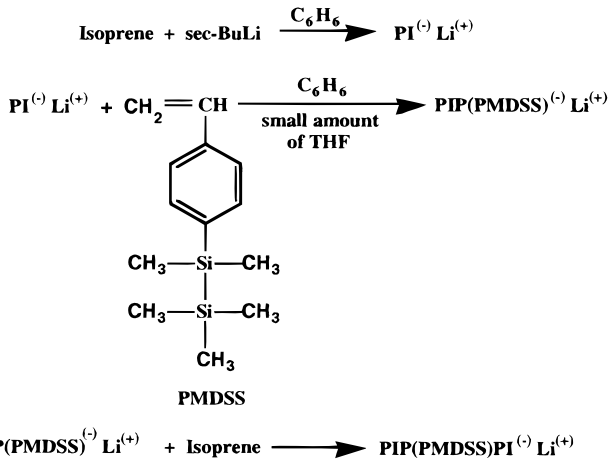

activated with 10 drops of 1,2-dibromoethane heated to a gentle reflux under nitrogen. *p*-Chlorostyrene (48 g, 346 mmol) was added slowly with efficient stirring until the mixture began to foam and reflux vigorously. Heating was discontinued and the remaining *p*-chlorostyrene was added at such a rate that continuous refluxing was maintained. After the addition, the mixture was heated to reflux for another 40 min. Chloropentamethyldisilane (36.1 g, 216 mmol) in THF (50 mL) was added at 35 °C and the final mixture was heated at 50 °C for 1 h. The cooled mixture was diluted with hexane and filtered through Celite. Solvent was evaporated under vacuum and the crude product was column chromatographed with petroleum ether. The final product was distilled, giving a clear oil 35.6 g (70%): bp 72−74 °C, (0.5 mTorr); ^{1}H NMR δ ($CDCl_3$) 7.30−7.38 (m, 4H), 6.65 (dd, 1H, J = 17.61, 10.87 Hz), 5.71 (dd, 1H, J = 0.94, 17.66 Hz), 5.18 (dd, 1H, J = 0.94, 10.86 Hz), 0.27 (s, 6H), 0.91 (s, 9H); ^{13}C NMR δ($CDCl_3$) 139.4, 137.5, 136.9, 134.0, 125.5, 113.8, −2.3, −4.0.

(b) Synthesis and Molecular Characterization of the Triblocks. The procedure used for the synthesis of the PMDSS block is very similar to that of Hirao's as described in ref 26, as seen in Scheme 1.

p-Pentamethyldisilylstyrene (PMDSS) was purified following typical procedures for styrene. Monomer was distilled from CaH_2 to dibutylmagnesium and then to ampules which were used for the polymerizations. The distillation of PMDSS was carried out at temperatures higher than those used for the distillation of simple styrene monomer, since the boiling point of PMDSS (72 °C at 0.5 mmHg) is higher than that of styrene (∼50 °C at 0.5 mmHg). It was found that the monomer behaved exactly like styrene during the synthesis, since the polydispersity index of a homopolymer P(PMDSS) was very low (1.06) and the observed molecular weight (M_w) of 37 K was very close to the expected molecular weight of 34 K. The difference between the predicted and actual molecular weights is well within the experimental errors of the two characterization methods, low angle laser light scattering (LALLS) and size exclusion chromatography (SEC).

SEC experiments were carried out at 30 °C using a Waters model 510 pump, Waters model 410 differential refractometer, and Waters model 486 tunable absorbance detector. Three Phenomenex (type, phenogel 5 linear; pore size, 50 to 10^6 Å) columns were used. THF, distilled over CaH_2 and sodium, was the carrier solvent at a flow rate of 1 mL/min.

The weight-average molecular weight ($\overline{M}_w$) of the final polymers was determined with a Chromatix KMX-6 low-angle laser photometer (LALLS). This instrument, equipped with a helium−neon laser, was operated at a wavelength of 633 nm. The refractive index increments, dn/dc, in THF at 25° C were measured with a Chromatix KMX-16 refractometer.

The $\overline{M}_w$ values were obtained from the $(KC/\Delta R_\theta)^{1/2}$ vs C plots (ΔR_θ, excess Rayleigh ratio; K, combination of known optical constants; C, concentration). In all cases the correlation coefficient was better than 0.99.

^{1}H NMR determination of the composition and the microstructure of the materials was carried out in $CDCl_3$ at 30 °C using a Varian Unity Plus 300/54 instrument.

(c) Sample Preparation. Samples were prepared by casting ∼5% w/w solution of the polymers in toluene, for a week at room temperature. (Since the solubility parameter of PMDSS is presently not known, toluene was used, and judging from the microphase separation from the TEM micrographs, it was an appropriate solvent.) After casting, the polymer films were approximately 0.7 mm thick. They were then annealed in a vacuum oven at 120 °C for 7 days.

(d) Morphological Characterization. To study the bulk-cast films by transmission electron microscopy, films approximately 500−1000 Å thick were sectioned at −90 °C using a diamond knife equipped Reichert-Jung 4E cryo-ultramicrotome. The polymer sections were then picked up on both 600-mesh copper grids and onto carbon films on 100-mesh copper grids, and the polyisoprene blocks were preferentially stained in vapors of a 4% osmium tetroxide water solution for 2 h. The films were then characterized in the bright field mode using a JEOL 2000FX transmission electron microscope, operating at 200 kV, unless otherwise noted. A goniometer stage with a double tilt holder was used to obtain high-symmetry 2-D projections of the morphology.

The space group of the cubic structure was investigated by obtaining diffraction patterns of the negatives using an optical diffractometer equipped with a 5 mW polarized UniPhase helium−neon laser with λ = 633 nm. Polaroid film was exposed for 1/16 s to record the optical diffraction images. Up to fourth-order peaks were seen in the optical transforms of the negatives and these correlated well to the computer simulated fast Fourier transforms (FFTs) of the digitized images. FFTs were made from the TEM images, using a montage of 32 × 32 unit cells in a 1024 × 1024 pixel array. A program written by Dr. R. Lescanec uses the 1024 × 1024 input and multiplies it by a Hanning window to reduce edge effects in the FFT. This program performs the FFT and outputs the data on a log scale as a 2-D image. X-ray diffraction data (SAXS) were acquired at the Time-Resolved Facility (station X12B) at the National Synchrotron Light Source at Brookhaven National Laboratory (BNL). There are no characteristic low-angle Bragg peaks despite the extremely good microdomain order observed in TEM. This is simply due to the fact that PI and P(PMDSS) have almost equal densities,[29] resulting in poor contrast between the two blocks and therefore very weak scattering. Due to the excellent order of the 24/100/26 PI/P(PMDSS)/PI sample, the characterization of the microdomain morphology is possible by combining TEM, optical diffraction patterns, and digitized FFTs.

(e) Reactive Ion Etching and Ozonolysis. Oxygen reactive ion etching was performed on the P(PMDSS) homopolymer and a PS homopolymer. Solutions of the polymers (5 wt %) were made in toluene and spun onto 1 in. silicon wafers still containing their native oxide. The thicknesses of the PS, P(PMDSS), and P(PMDSS)/PI/P(PMDSS) samples were 850, 200, and 240 nm, respectively. The etching experiments were carried out in a low-pressure, magnetically enhanced inductively coupled plasma etcher. Etching was performed with a base pressure of 10 mTorr and an oxygen flow rate of 40 cm^2. The top radio frequency generator was set at 250 W and the bottom radio frequency generator at 50 W. Etching was carried out at 0 °C for 60 s. Etch rates were calculated by measuring film thickness before and after etching using a profilometer.

Sections of the 24/100/26 PI/P(PMDSS)/PI, as prepared by microtoming, were exposed to a flowing 2% ozone atmosphere for 1 h at room temperature in order to preferentially oxidize the polyisoprene block. The PI-oxidized fragments were then

(29) The density for various components (in g/cm^3) is ρ_{PS} = 1.05, ρ_{PI} = 0.913, as reported in the *Polymer Handbook*, and $\rho_{P(PMDSS)}$ = 0.915, as calculated by X-ray reflectivity at IBM. Since the density difference between the PI and P(PMDSS) blocks is so small, no contrast is seen by SAXS.

removed by soaking the samples in deionized water overnight and the samples examined under TEM at 100 keV.

Results and Discussion

The synthetic procedure described here is the sequential addition of the monomers.

Following the synthesis of the polyisoprenyllithium block, a small amount of THF (0.5 mL) was added in order to promote the initiation of the poly(pentamethyldisilylstyrene) block and maintain the narrow molecular weight distribution of the diblock precursor. It should be noted that in the final block copolymer, the two PI end blocks have different molecular weights and different microstructures. The difference in microstructure was determined from ^{1}H NMR spectroscopy and can be attributed to the small amount of the polar solvent THF that was added in the synthesis of the second PI block. The first PI block, which was synthesized in pure benzene, has a microstructure that is typical of anionic polymerization of isoprene in a nonpolar solvent (10 wt % 3,4, 70 wt % cis-1,4 and 20 wt % trans-1,4). However, since the second block was synthesized in benzene with a small amount of a polar solvent, the microstructure contains 1,2-microstructure and an increased value of 3,4-microstructure (8 wt % 1,2, 42 wt % 3,4, and 50 wt % 1,4). Since only a small amount of THF was present during the synthesis, the 1,2-content is not as high as isoprene polymers synthesized in strictly polar solvents, but there was a significant increase in the 3,4-component.

The mixture was allowed to react for 3 h at 40 °C to complete the polymerization of the middle PMDSS block. Before adding the third monomer (isoprene), an aliquot of the diblock was taken for characterization by GPC. It is known from anionic polymerization of styrene and isoprene that the colors of the living end change during polymerizations, depending on the monomer that is being polymerized. In the case of styrene, a dark red-orange color is normally present (depending on the molecular weight of the polymer and the concentration of the solution), while for isoprene, a yellow to pale yellow color is usually observed. The change from one color to the other, when the appropriate monomer is added, should be nearly instantaneous since the initiation and propagation rates are fast in both cases. Despite the fact that in PMDSS the side group on the phenyl ring is large (which could contribute to steric hindrance, thereby decreasing the initiation rate), the color change from yellow to orange was indeed nearly instantaneous with the addition of THF. The incorporation of a small amount of polar solvent leads to a decrease in the degree of aggregation of the solution from 3−4 to 2.[30] It is important to note that when the isoprene monomer was added to the P(PMDSS) living end, the change in color from orange to yellow was very slow, leading to the conclusion that the P(PMDSS)$^-$Li$^+$ is a poor initiator for the polymerization of isoprene.

In the P(PMDSS)-rich sample, due to possible impurities in the PMDSS monomer, a small percentage of the first block, PI$^-$Li$^+$, was terminated. This is shown in Figure 2 at the chromatograph of the PI-*b*-P(PMDSS) living end and it is characterized as "terminated" PI arm. Fractionation was carried out by adding methanol (nonsolvent) to the stirred polymer solution (~0.5% w/v) in toluene (solvent) at room temperature until turbidity was detected. The mixture was then heated and stirred until clear, transferred to a warm separatory funnel, and allowed to equilibrate to room temperature overnight. The procedure continued until the undesirable products were no longer present by using SEC. Typical SEC chromatographs of the precursors and the unfractionated and the fractionated triblocks are given in Figure 2. The molecular characteristics of the two triblocks are shown in Table 1.

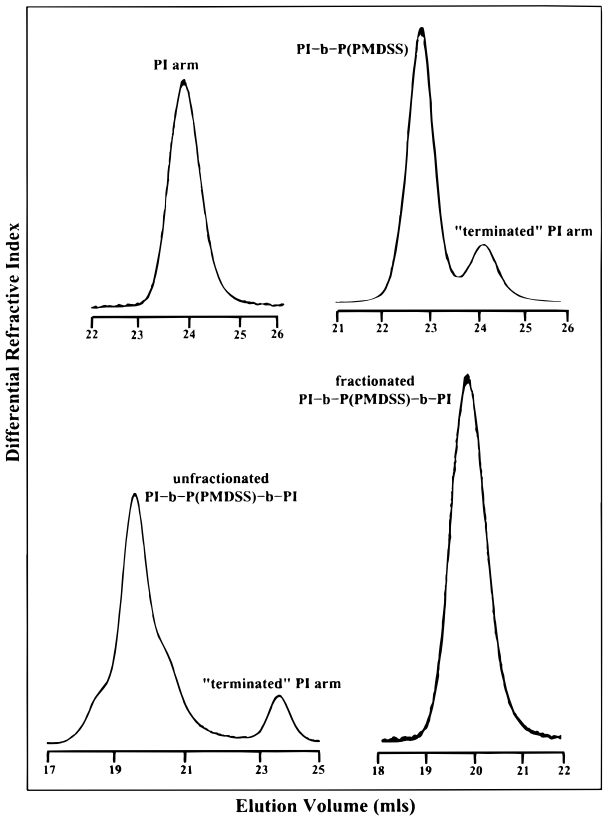

Figure 2. SEC chromatographs for the 24/100/26 PI−P(PMDSS)−PI sample.

Table 1. Molecular Characteristics of the Precursors and the Final Polymers

sample	M_w[a] × 10^{-3} (g/mol)	M_w/M_n	wt % PI	
			^{1}H NMR	calcd
PI	24.3	1.05		
PI-*b*-P(PMDSS)	123.1	1.10	0.18	0.20
PI-*b*-P(PMDSS)-*b*-PI	149.3	1.12	0.36	0.35
P(PMDSS)	52.2	1.07		
P(PMDSS)-*b*-PI	302.4	1.14	0.80	0.83
P(PMDSS)-*b*-PI-*b*-P(PMDSS)	345.2	1.24	0.74	0.73

[a] From low-angle laser light scattering (LALLS) in THF at 25 °C.

For the BAB PI-rich copolymer, the reactions used were similar to the above reactions, except that the order of monomer addition is reversed. In this polymerization, the small amount of THF which is needed to enhance reaction kinetics is added just before the polymerization of the final PMDSS end block, after the middle PI block has been polymerized. For this reason, the microstructure of the PI is characteristic of anionic polymerization of isoprene in a nonpolar solvent.

(30) Morton, M.; Fetters, L. J. *Rubber Chem. Technol.* **1975**, *48*, 359.

This behavior is completely different from that of the PS^-Li^+ living end, where the initiation of isoprene is essentially instantaneous. This slow initiation explains the increased polydispersity of the P(PMDSS)/PI diblock shown in the SEC chromatographs. To overcome this slow initiation and obtain low polydispersity of the final polymer, a small amount of a polar component should be added to increase the initiation and propagation rate of the isoprene block by the $P(PMDSS)^-Li^+$. However we chose not to do that in order to avoid obtaining a PI block with high 3,4-microstructure. It should be noted that the polydispersity of the P(PMDSS)−PI−P(PMDSS) block copolymer is higher than usual due to the high molecular weight of the PI block (approximately 250 000). This high molecular weight coupled with a solution concentration of ~20% resulted in a viscous solution.

Since the half-life ($t_{1/2}$) of PI is 1 h and the polymerization is considered to be completed in $6t_{1/2}$, THF was added after 10 h to increase the solubility of the solution and help the polymerization of the final block. By waiting such a long time, the change in microstructure of the PI block was negligible. From ^1H NMR spectroscopy it was determined that the microstructure adopted by the PI block was typical for the anionic polymerization of isoprene in benzene.

Structural Characterization

The morphologies of the two triblocks were determined by TEM. The sample with the PI midblock exhibits disordered light spheres of P(PMDSS) in a dark OsO_4-stained PI matrix (Figure 3a). The morphology of the P(PMDSS)-rich sample is shown in Figure 3b. The PI, which is selectively stained with OsO_4, is the minority phase and forms two dark interpenetrating networks within a P(PMDSS) matrix. The molecular weight of this copolymer is approximately half of the aforementioned triblock and exhibits excellent long-range order even in the unannealed state. Figure 3b shows 6-fold symmetric grains after annealing the P(PMDSS)-rich sample at 120 °C for 7 days. The grain sizes observed in the cubic sample were much larger than those observed in analogous triblock PS−PI−PS polymers.[31] For example, in well-annealed PS-*b*-PI-*b*-PS samples of comparable total molecular weight, the grain sizes varied from 20 × 20 to 30 × 30 unit cells, but in this case they are at least 50 × 50 unit cells.

Transmission Electron Microscopy, Optical Diffraction Patterns, and Fast Fourier Transforms. *Six-Fold Projection.* The appearance of "wagon-wheel" structures in the ⟨111⟩ projection has previously caused confusion in the morphological identification of block copolymers with cubic structures. In Figure 4a,b the TEM image with *p*6*mm* symmetry and the digitized FFT of the TEM image are exhibited. Higher order peaks are evident in the FFT transforms. There are strong similarities of the image and its FFT to those exhibited earlier by Avgeropoulos et al.,[31] for a PS−PI−PS triblock of similar composition. The main difference between the two polymers is the position of the PI block. The two Fourier transform patterns each have 12 prominent peaks around the center beam, with an alternating pattern of a high-intensity peak next to a lower intensity peak. The higher intensity peaks occur at a smaller q than the lower intensity ones, and the q_2/q_1 ratio is approximately equal to 1.15 in both transforms. The experimental ratio agrees very well with the theoretically determined ratio ($1.165 = q_{220}/q_{221} = \sqrt{8}/\sqrt{6}$) for a sample exhibiting double gyroid morphology with *Ia*3*d* space group symmetry. The peaks in the FFT are indexed according to the DG model. The best agreement of simulated images with the TEM data occurs for models with a section thickness of about 1 unit cell.

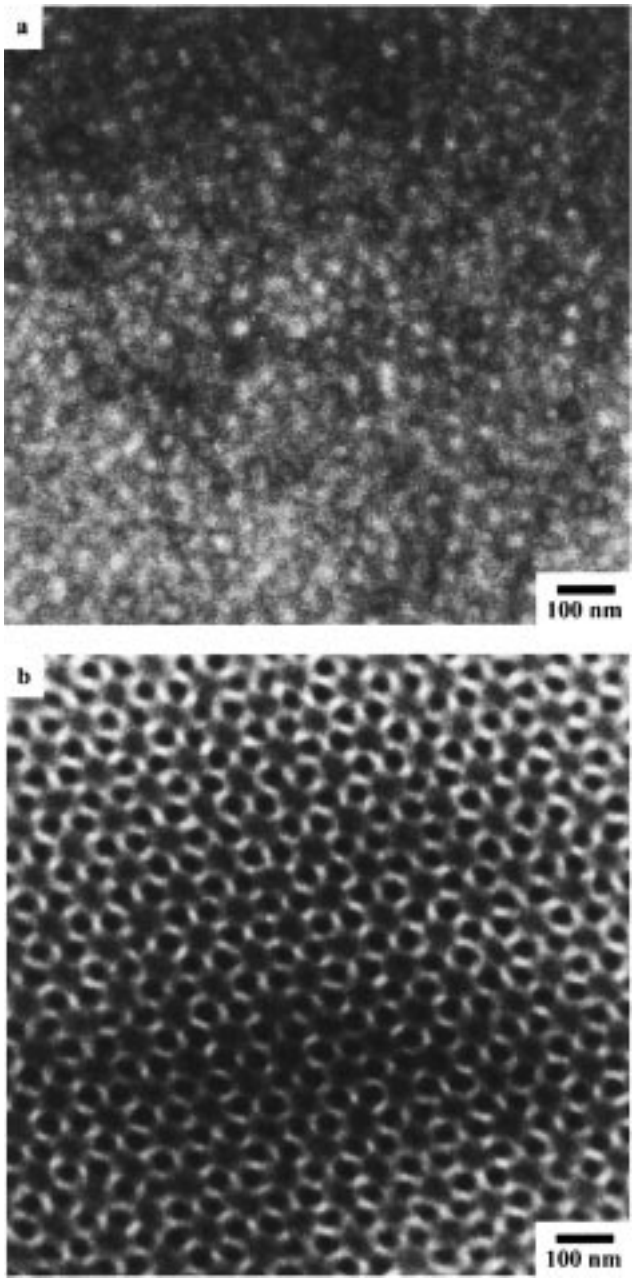

Figure 3. (a) Bright-field TEM image of the 52/250/42 P(PMDSS)−PI−P(PMDSS) triblock exhibiting spherical morphology. The PI matrix is stained with OsO_4, so it appears dark. (b) Bright-field TEM image of the 24/100/26 PI−P(PMDSS)−PI sample exhibiting the [111] projection of the P(PMDSS)-rich sample (wagon-wheel projection). The sections were stained with OsO_4, so the minority PI networks appear dark.

(31) Avgeropoulos, A.; Dair, B. J.; Hadjichristidis, N.; Thomas, E. L., *Macromolecules*, **1997**, *30*, 5634.

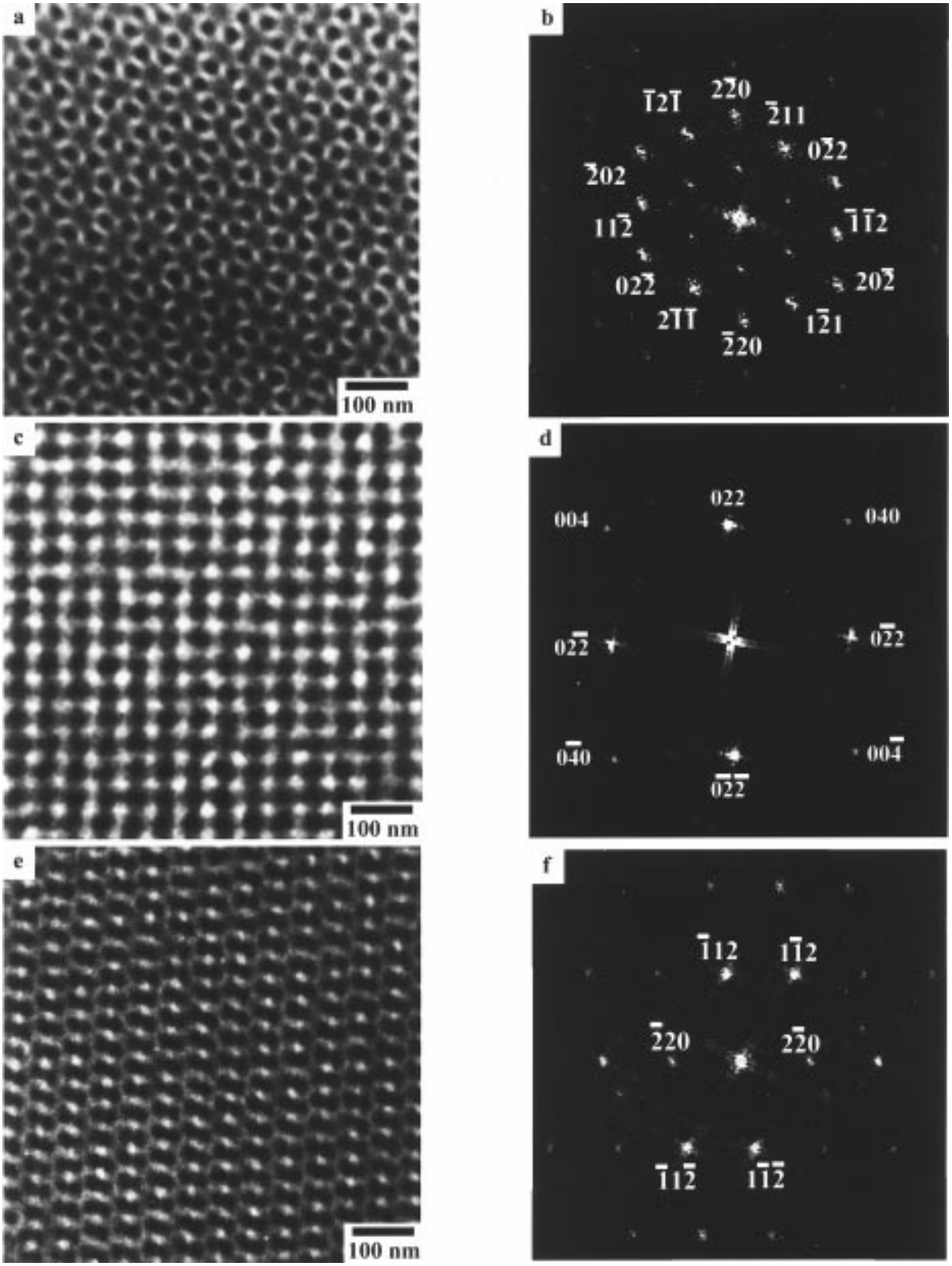

Figure 4. TEM images of 24/100/26 PI/P(PMDSS)/PI. (a) Bright-field TEM image exhibiting the [111] projection. (b) Indexed digitized FFT of the TEM image. (c) Bright-field TEM image exhibiting the [100] projection. (d) Indexed digitized FFT of the TEM image. (e) Bright-field TEM image exhibiting the [110] projection. (f) Indexed digitized FFT of the TEM image.

*Four-Fold Projection***.** Figure 4c,d shows the TEM image, exhibiting *p*4*mm* symmetry, and the digitized FFT pattern. The angle between the first-order diffraction peaks was measured to be 89°, indicating that the projection is almost perfectly down the 4-fold axis. The FFT also indexes well according to the DG model.

*Two-Fold Projection***.** The ⟨110⟩ projections of the DG have *c*2*mm* plane group symmetry. Figure 4e,f shows the TEM image and the digitized FFT, all exhibiting *c*2*mm* symmetry. The 2-fold projections are the eluci-

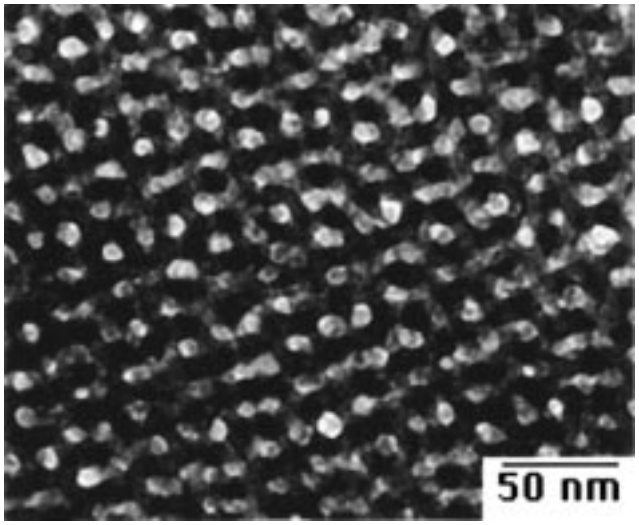

Figure 5. Bright-field TEM of the unstained double gyroid sample after exposure to an ozone atmosphere for 1 h. Contrast is due to the removal of the PI channels.

dative cubic symmetry projections for identifying the DG morphology compared to structures based on other cubic space groups. The resemblance between the present set of images and those obtained in an earlier work[31] for the PS-rich triblock copolymer leads to the conclusion that the morphology observed is DG.

Ozonolysis and Reactive Ion Etching

When thin films of a bulk sample containing the tricontinuous morphology were exposed to ozone, the polyisoprene block was preferentially removed. The contrast in Figure 5 arises from the selective removal of the PI regions. This nanoporous structure is similar to that very recently reported in ozone-etched PI/PS/PI triblock copolymers by Hashimoto et al.[20] Both extensive selective reactive ion etching and ozonolysis studies (separately and in concert) on the double gyroid morphology are in progress and will be reported in detail at a later time.

The O_2-RIE etch rates of films of the PS and P(PMDSS) homopolymers were approximately 800 and 15 nm/min, respectively, resulting in an etch selectivity of approximately 50:1. It should be noted that etch times longer than 60 s could not be carried out because the PS would be completely removed by the oxygen plasma. PS rather than PI was used for the homopolymer etching studies because of the low glass transition temperature of PI, which would prevent the use of profilometry for the calculation of etch rates. Since the oxygen plasma reacts with the carbon atoms, the etch rate of PS and PI will be very similar. For example, Wolf and Taylor have shown that the etching rate of cross-linked PI relative to PS is approximately 5.55:1.[32] It should be noted though, that this relative rate is calculated using different etching conditions and on a different reactor than used in our studies.

Preliminary etching work was also carried out on both block copolymer samples under the experimental conditions used to etch the homopolymers. A nanoporous double gyroid morphology is also present in the O_2-RIE samples, although the images are less well defined than for the ozone etching. Since RIE is generally an anisotropic process, more extensive studies are needed to be carried out in order to produce a more isotropic plasma. This is achieved by utilizing lower bias voltages and higher gas pressures, and the details will be reported later.

Conclusions

The synthesis and the morphology of two triblock copolymers of the type ABA and BAB, where A is polyisoprene and B is poly(pentamethyldisilylstyrene), are reported. Through TEM images and their fast Fourier transforms, the 64% P(PMDSS) sample was determined to have a PI double network gyroid structure with *Ia*3*d* space group symmetry and the 26% P(PMDSS) sample was disordered spherical domains of P(PMDSS). Preliminary selective oxidation of the PI phase in the double gyroid with ozone delineates the bulk morphology. These block copolymers should have a high potential for the formation of nanostructures by O_2-RIE and/or ozonolysis, because unlike currently available block copolymers, the silicon is not only in the high T_g phase but is present in the monomer, so postchemistry after polymerization is unnecessary. Future work will be done on these polymers to study their oxidative imaging by O_2-RIE and ozonolysis separately and in concert to determine their viability as materials for different nanoporous applications.

Acknowledgment. We would like to thank Dr. M. Capel for his technical assistance at the National Synchrotron Light Source at Brookhaven National Laboratory and Dr. R. Albalak for his help in the X-ray facility located at the Center for Materials Science and Engineering at MIT. The authors would also like to thank Dr. M. Tomey at IBM for his help with X-ray reflectivity measurements. This project was supported by ACS PRF No. 30050-AC7, AFOSR ASSERT No. F49 620-94-1-0357. V.Z.C. would like to thank the National Science Foundation and IBM for graduate research fellowships and acknowledges partial support for this work from the NSF Center for Polymer Interfaces and Macromolecular Assemblies (CPIMA) at IBM.

CM970682Y

(32) Taylor, G. N.; Wolf, T. M. *Polym. Eng. Sci.* **1980,** 20, 1087.